Eur Radiol (2005) 15: 2513–2524
DOI 10.1007/s00330-005-2852-4



**R. Schmitt**
**G. Coblenz**
**O. Cherevatyy**
**H. Brunner**
**S. Fröhner**
**E. Wedell**
**G. Karg**
**G. Christopoulos**

# Comprehensive MR angiography of the lower limbs: a hybrid dual-bolus approach including the pedal arteries

Received: 22 December 2004
Revised: 8 June 2005
Accepted: 24 June 2005
Published online: 22 July 2005


R. Schmitt (✉) · G. Coblenz · O. Cherevatyy · H. Brunner · S. Fröhner · E. Wedell · G. Christopoulos
Diagnostic and Interventional Radiology, Herz- und Gefäßklinik GmbH, Salzburger Leite 1, 97616 Bad Neustadt an der Saale, Germany
e-mail: schmitt.radiologie@herzchirurgie.de
Tel.: +49-9771-662901
Fax: +49-9771-659215

G. Karg
Siemens Medical Solutions, Erlangen, Germany

**Abstract** The purpose of this study was to include the pedal vasculature into the coverage of peripheral multistation magnetic resonance angiography (3DceMRA). A total of 216 patients suffering from peripheral vascular disease were examined with a modified hybrid dual-bolus technique. The cruropedal arteries were acquired first with two sagittal slabs and time-resolved 3D sequences. Then the aortofemoral vessels were visualized using the bolus-chase technique and a second contrast injection. Interventional procedures were performed in 104 patients, and in 69 of those, the cruropedal vessels were also examined with digital subtraction angiography (iaDSA). Using 3DceMRA, the cruropedal arteries were displayed with both excellent and good quality in 95% (205/216 cases), and without any venous overlay in 94% (203/216 cases). The aortofemoral vessels were not jeopardized by the first contrast injection. With iaDSA as the standard of reference, observed sensitivity of 3DceMRA was found in ranges from 80% (29%, 99%) to 100% (86%, 100%) for assessing significant stenoses, and observed specificity ranged between 93% [80%, 98%] and 100% (82%, 100%). In conclusion, hybrid dual-bolus 3DceMRA significantly reduces the limitations of standard single-bolus 3DceMRA in anatomic coverage and temporal resolution of the cruropedal arteries, thus providing high-quality images of the entire peripheral vasculature.

**Keywords** Angiography, comparative studies · Arteries, peripheral · Arteries, stenosis or obstructions · Arteriosclerosis · Magnetic resonance (MR), vascular studies

## Introduction

In recent years, contrast-enhanced magnetic resonance angiography (3DceMRA) has emerged as a reliable, noninvasive tool in assessing peripheral vascular disease (PVD) of the lower limbs [1–4]. Multistation acquisition of the peripheral arteries is possible with high-performance gradient systems, ultra-fast 3D sequences, automatic movement of the patient table [5], techniques of bolus detection [6], optimized 3D volume placement with flexible choice of scan parameters [7], and the use of dedicated multichannel phased-array coils [8–10]. Sensitivity and specificity rates between 81 and 100% have been reported for the detection of significant stenoses in comparison to catheter angiography, which is regarded as the standard of reference [3, 4, 11, 12]. Two problems could potentially arise in multistation 3DceMRA with the standard craniocaudal acquisition order ("bolus-chase" 3DceMRA).

Firstly, assessment of crural arteries may be limited due to early filling of adjacent veins [2, 11, 13]. This happens when cellulitis and diabetic ulcera shorten the arteriovenous transit time of the contrast agent [13–15]. To over-

come this phenomenon, positioning of the calves without muscle compression [1], venous compression at the mid-femoral level [16], a step-by-step technique with repeated contrast injections [17, 18], the use of parallel imaging techniques like SENSE [19, 20], and hybrid approaches [15, 21–23] have been recommended. The hybrid approach is a dual-bolus technique for acquiring the crural station first, and then adding a two-station bolus-chase 3DceMRA to cover sequentially both the pelvic and femoral stations [15, 21].

Secondly, coronal acquisition of the crural arteries using a slab thickness of 60 to 90 mm does not always cover the pedal arteries [24]. If patency of the pedal arteries is of strategic interest in planning a percutaneous intervention or distal bypass grafting, the 3DceMRA scan strategy has to be changed at the cruropedal station either by increasing the anteroposterior thickness of the coronal slab as described for the bolus-chase approach [4, 10, 20], or by performing a dedicated 3DceMRA acquisition of the feet with coronal [24] or sagittal slabs [25, 26].

The aim of our study was to include the pedal arteries in a comprehensive, multistation, 3DceMRA technique of the lower limbs. Therefore, we refined the hybrid approach mentioned above. In our modified technique, the cruropedal vessels of both legs were covered with two sagittal slabs and were acquired with a time-resolved sequence.

## Materials and methods

From the beginning of July 2004, we changed the acquisition strategy of contrast-enhanced MR angiography (ceMRA) of the lower limbs. In our routine work-up, all consecutive ceMRA examinations were performed in a refined way described as follows.

### Patients

During a 10-week period (15 July 2004 to 30 September 2004), all consecutive patients referred for ceMRA of the lower limbs were included into the retrospective analysis.

*Entire patient group* A total of 216 patients (70 women, 146 men; mean age 69±11 years) suffering from symptomatic peripheral vascular disease underwent 3DceMRA of the lower limbs. Fontaine's classification was for stage I: no case, stage IIa: 26 cases, stage IIb: 94 cases, stage III: 26 cases, and for stage IV: 70 cases (see Table 1). Written informed consent was obtained from all patients.

*Patient subgroup 1* This subgroup consisted of 69 patients selected on the basis of available intra-arterial angiograms (iaDSA) that were carried out either before percutaneous transluminal angioplasty (PTA) of the crural arteries (19 cases), or after PTA of a iliacal or femoropopliteal arteries to document the absence of PTA-associated embolism (50 cases). In 6/69 bilaterally treated patients, only the first procedure was selected for evaluation in each case. Fontaine's classification is listed in Table 1.

### Hard- and software

3DceMRA examinations were performed on two 1.5 T MR scanners equipped with either 20 mT/m ("scanner 1") or with 40 mT/m ("scanner 2") gradient systems (Magnetom Symphony and Magnetom Sonata, Siemens Medical Solutions, Erlangen, Germany). For covering Z-axis anatomy from the diaphragm down to the feet, a dedicated 12-element phased-array coil (Siemens Medical Solutions, Erlangen, Germany) was used in combination with a body

**Table 1** Demographical data of the patients included in the study

| Demographical data | Entire patient group (ceMRA only) | Patient subgroup 1 (ceMRA+iaDSA) | Patient subgroup 2 (remaining) | Statistics (comparison between subgroup 1 and 2) |
|---|---|---|---|---|
| Number of patients (*n*) | 216 | 69 | 147 | |
| Gender (*n*) | 70 females<br>146 males | 18 females<br>51 males | 52 females<br>95 males | NS ($p$=0.17)[a] |
| Age (m±SD) | 69±11 | 67±10 | 70±11 | NS ($p$=0.07)[b] |
| Fontaine's stage I (*n*) | 0 | 0 | 0 | NS ($p$=0.78)[a] |
| Fontaine's stage IIa (*n*) | 26 | 6 | 20 | |
| Fontaine's stage IIb (*n*) | 94 | 31 | 63 | |
| Fontaine's stage III (*n*) | 26 | 9 | 17 | |
| Fontaine's stage IV (*n*) | 70 | 23 | 47 | |

The patient cohort consisted of 216 individuals, all of them examined with 3DceMRA. In 69 of these patients (subgroup 1), intra-arterial catheter angiograms (iaDSA) were performed during interventional therapy, but not in the remaining 147 individuals (subgroup 2). *NS* not significant

[a] Both subgroups were statistically analyzed using the chi$^2$-test for descriptive testing of differences between groups (frequencies)

[b] Both also were analyzed using the Mann-Whitney U test for descriptive testing of differences between groups (continuous data)

phased-array coil connected to spine coil elements. The latter were connected to a large FOV extender [27]. No additional coil was used for pedal coverage, thus the toes remained outside the coil (Fig. 1a). The contrast agent and saline solution were administered intravenously with a MR-compatible power injector (Spectris, Medrad, Indianola/USA).

## Contrast agent

A total of 18 ml of gadobenate dimeglumine (Gd-BOPTA, Multihance, Bracco ALTANA Pharma GmbH, Konstanz, Germany) was administered in a dual-injection technique. After the nonenhanced data set of the cruropedal region had been acquired, 7 ml of Gd-BOPTA was injected at a flow rate of 1.0 ml/s followed by 20 ml of a saline flush at the same flow rate. A second injection of 11 ml Gd-BOPTA (consisting of 6 ml at a flow rate of 1.0 ml/s, and 5 ml at a flow rate of 0.3 ml) and 20 ml of a saline flush at a flow rate of 0.3 ml were administered after nonenhanced data sets of the thigh/knee and pelvic regions had been acquired.

## MR angiographic technique

Patients were positioned feet first on a table equipped with an automated moving device. Both lower limbs, including the feet, were secured with straps in the 12-channel-coil device to minimize movement artifacts (Fig. 1a). The examination commenced at three/(four) stations with triplane localizers using TrueFISP sequences to prescribe the 3D slabs of nonenhanced and contrast-enhanced multistation sequences. A dual-bolus technique was applied (Fig. 1b).

To achieve anatomic coverage of the feet and distal calves (cruropedal station), two separate (right and left) slabs were acquired in sagittal orientation using an ultrafast, T1-weighted, spoiled 3D-fast low-angle shot (FLASH) sequence. An initial nonenhanced ("mask") data set was

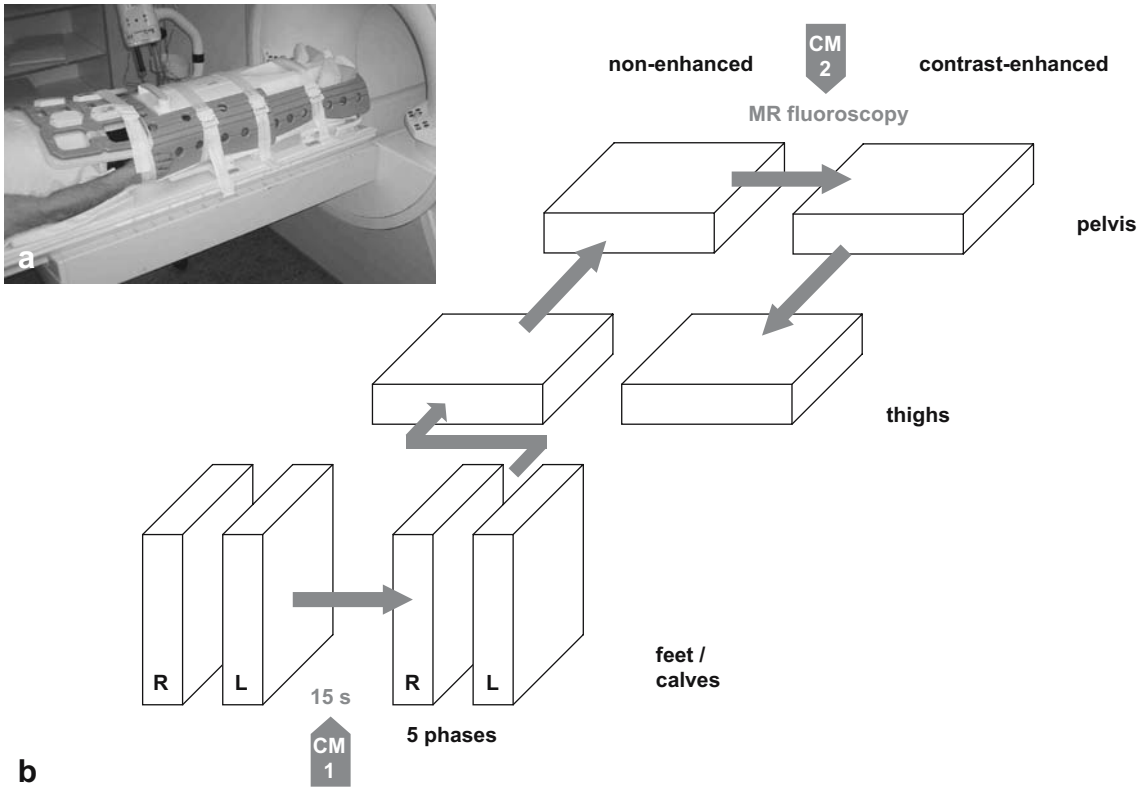


**Fig. 1** Modified hybrid 3DceMRA technique. Left upper corner: Coil setup with the patient outside the scanner. Both, the body phased-array coil (*left*) and the peripheral 12-element phased-array coil (*right*) are applied. Diagram with *arrows* indicating the acquisition order: nonenhanced data set of the distal calves and feet (sagittal, each side separate), followed by injection of the first amount of the contrast agent (CM1), followed by fixed delay of 15 s, followed by contrast-enhanced data sets of the distal calves and feet (five sagittal phases each), followed by nonenhanced data set of the knees and distal thighs (coronal), followed by nonenhanced data set of pelvis and the proximal thighs (coronal), followed by injection of the second amount of the contrast agent (CM2), followed by MR fluoroscopy of the contrast arrival, followed by contrast-enhanced data set of the pelvis and the proximal thighs (coronal), followed by contrast-enhanced data set of the distal thighs and knees (coronal)

acquired, followed by the injection of 7 ml contrast agent. After a fixed time delay which was set to 15 s in all patients, five dynamic contrast-enhanced data sets were acquired continuously. Data sets of the right and left slabs were obtained with an alternating slice measuring order (measuring the right slab for 10 s, then the left slab for 10 s, ...). The k-space filling was centric. A modified SENSE technique (GRAPPA) with a two-fold reduction was applied on both scanners. Acquisition time of each phase took 20 s. The FOV was 450 mm on scanner 1, and 400 mm on scanner 2, each with rectangular sizes of 62.5%. The slabs were covered by 36 partitions of 2.4 mm thickness, interpolated to 1.2 mm (scanner 1), and by 40 partitions of 1.8 mm thickness, interpolated to 1.2 mm (scanner 2), respectively. To maintain identical acquisition times on both scanners, the acquisition matrix was set to 384×178 (scanner 1) and 512×288 (scanner 2), yielding acquired voxel resolutions of 1.6×1.2×2.0 $mm^3$ and 0.9×0.8×1.8 $mm^3$, respectively. The other parameters are summerized in Table 2.

After finishing the cruropedal acquisition, a bolus-chase approach was performed from the suprarenal abdominal aorta level down to the tibial trifurcations. The aorto-femoropopliteal length was covered with two consecutive and overlapping stations on scanner 1, and with three stations on scanner 2, respectively. The reduced FOV of 400 mm required a three-station approach on scanner 2, whereas the FOV of 450 mm enabled a two-station bolus-chase on scanner 1. At these levels, an ultra-fast, T1-weighted, spoiled 3D-fast low-angle shot (FLASH) sequence was applied with centric k-space filling. The nonenhanced run was performed in the thigh-to-abdomen direction, followed by the contrast-enhanced run in the abdomen-to-thigh direction at each station with an overlap of 60 mm (scanner 1) and 100 mm (scanner 2), respectively. For real-time monitoring of the contrast bolus arrival, the pelvic/abdomen scan was initiated every second by a MR fluoroscopic 2D sequence (CareBolus, Siemens Medical Solutions, Erlangen, Germany) acquired coronally through

**Table 2** Acquisition parameters of the 3D contrast-enhanced MR angiograms applied with two different scanners

| Scan parameter | 1.5 T, 20 mT/m Scanner | | | 1.5 T, 40 mT/m Scanner | | | |
|---|---|---|---|---|---|---|---|
| Station order | 1 | 2 | 3 | 1 | 2 | 3 | 4 |
| Station region | Foot/calf | Pelvis/thigh | Thigh/knee | Foot/calf | Pelvis | Thigh | Knee |
| Sequence type | FLASH 3D | FLASH 3D | FLASH 3D | FLASH 3D | FLASH 3D | FLASH 3D | FLASH 3D |
| Orientation | 2×sagittal | Coronal | Coronal | 2×sagittal | Coronal | Coronal | Coronal |
| Phase encoding | Ant-post | Right-left | Right-left | Ant-post | Right-left | Right-left | Right-left |
| Partitions (*n*) | 36 | 38 | 36 | 40 | 45 | 36 | 42 |
| FOV (mm) | 450 | 450 | 450 | 400 | 400 | 400 | 400 |
| Z-axis overlap/station | 0 | 60 | 60 | 0 | 100 | 100 | 100 |
| Rectangular FOV (%) | 62.5 | 75 | 75 | 62.5 | 87.5 | 81.3 | 81.3 |
| Slice thickness (mm)*a* | 1.2 | 1.4 | 1.4 | 1.2 | 1.4 | 1.4 | 1.2 |
| Slice encoding resolution (%)*a* | 60 | 63 | 60 | 67 | 63 | 60 | 75 |
| Partition thickness (mm)*a* | 2.0 | 2.22 | 2.33 | 1.8 | 2.22 | 2.33 | 1.6 |
| Voxel size ($mm^3$) | 1.6×1.2×2.0 | 1.0×0.9×2.2 | 1.7×1.2×2.3 | 0.9×0.8×1.8 | 1.0×0.8×2.2 | 1.3×0.8×2.3 | 1.0×0.8×1.6 |
| TR (ms) | 4.30 | 4.75 | 4.30 | 4.30 | 3.60 | 3.30 | 4.30 |
| TE (ms) | 1.53 | 1.87 | 1.56 | 1.32 | 1.32 | 1.07 | 1.39 |
| Flip angle (°) | 25 | 25 | 25 | 30 | 30 | 30 | 30 |
| Time to k-space middle (s) | 0.5 | 0.5 | 0.5 | 0.5 | 0.5 | 0.5 | 0.5 |
| Band width (Hz/Px) | 420 | 340 | 360 | 330 | 390 | 390 | 340 |
| Acquisitions (*n*) | 2×1 | 1 | 1 | 2×1 | 1 | 1 | 1 |
| Acquisition time (s) | 2×10 | 16 | 20 | 2×10 | 16 | 20 | 21 |
| Large FOV filtering | Yes | Yes | Yes | Yes | Yes | Yes | Yes |
| Coil elements (*n*) | 4 | 8 | 6 | 4 | 7 | 9 | 6 |
| Resolution fr×ph (Px) | 384×178 | 512×330 | 384×199 | 512×288 | 512×336 | 512×250 | 512×312 |
| Phase encoding resolution (%) | 74 | 86 | 69 | 90 | 75 | 60 | 75 |
| Phase partial Fourier (%) | 75 | 75 | 75 | 75 | 75 | 75 | 75 |
| Slice partial Fourier (%) | 75 | 75 | 75 | 75 | 75 | 75 | 75 |
| iPAT mode | GRAPPA 2 | GRAPPA 2 | None | GRAPPA 2 | GRAPPA 2 | None | GRAPPA 2 |

The protocol of the 1.5 T/20 mT/m scanner consists of three stations, whereas four stations are measured using the protocol of the 1.5 T/40 mT/m scanner. *FOV* Field of view, *fr* frequency direction, *GRAPPA* generalized autocalibrating partially parallel acquisition, *Hz* Hertz, *iPAT* integrated parallel acquisition technique, *n* number, *ph* phase direction, *px* pixel, *s* second

[a]Equation for thickness used: partition corresponds to slice/slice encoding resolution

the abdominal aorta. Thereafter, the table was automatically moved to the station of the thighs to acquire data of the femoropopliteal arteries. The time for interscan table movement was 4 s. Sensitivity encoding (GRAPPA) with a SENSE factor of 2 was applied at the pelvic station on both scanners, and at the popliteal station on scanner 2, but not at the height of the thighs. Acquisition parameters used in the individually tailored bolus-chase sequences on both scanners are listed in Table 2.

## Image postprocessing

Nonenhanced images were automatically subtracted from the corresponding contrast-enhanced images to remove background signals. For each station, 5 maximum-intensity projection (MIP) images were generated from the subtracted images in 45° rotational increments around a craniocaudal axis (Fig. 2) At the cruropedal station, at least two subsequent phases of both the right and left sides were selected from time-resolved data sets with respect to optimal vessel enhancement (Fig. 3), and MIP images of the different sides and phases were reconstructed separately. All MIP images were filtered for edge accentuation. While total acquisition time was approximately 20 min, time expense for postprocessing took an additional 10 min.

## Catheter angiograms

Catheter angiograms (iaDSA) of the nontreated cruropedal arteries were available in 69 of the 104/216 patients who underwent PTA procedures within a week. Intra-arterial digital subtraction angiography (iaDSA) of the distal calf

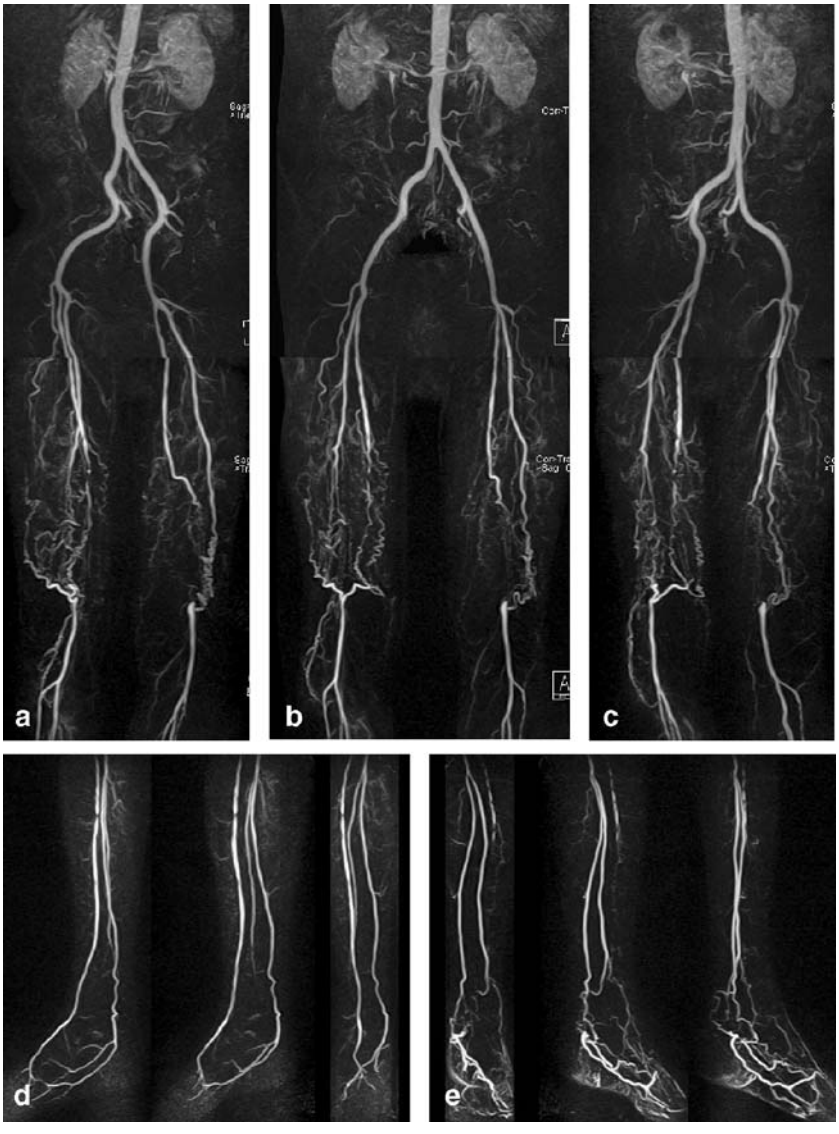


**Fig. 2** Modified hybrid 3DceMRA of an 80-year-old male suffering from bilateral claudication (Fontaine stage III). Aortofemoral bolus-chase 3DceMRA displayed with 45° oblique RAO (**a**), coronal (**b**) and 45° oblique LAO (**c**) maximum intensity projections. Bilateral occlusions of the superficial femoral arteries are evident. Plenty of collaterals have bilaterally filled the popliteal arteries and the patent trifurcation arteries. No overlaying veins are present. **d**– **e** Cruropedal time-resolved 3DceMRA, displayed in coronal, 45° oblique, and sagittal maximum intensity projections. On the *right side* (d), a solitary stenosis of the anterior tibial artery is present. On the *left side* (e), the anterior tibial artery is occluded proximally, and the posterior tibial artery distally. Collaterals originating from the peroneal and posterior tibial arteries have developed to supply the plantar vessels. At the sole of the foot, hyperemic soft-tissue areas are enhanced

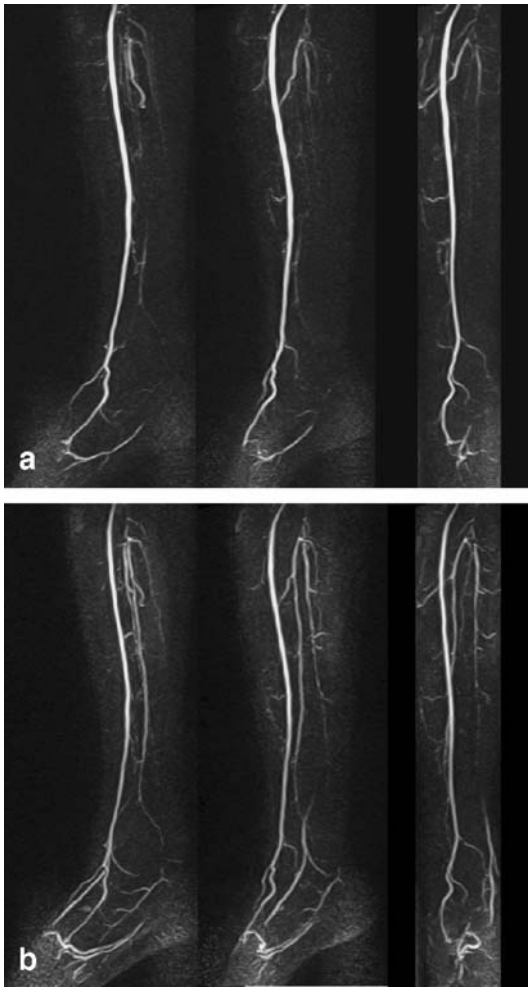


**Fig. 3** A 67-year-old diabetic male with a high-grade stenosis of the right tibioperoneal bifurcation. Two different phases of a cruropedal time-resolved 3DceMRA are displayed in coronal, 45° oblique, and sagittal maximum intensity projections. **a** In phase 2, only the anterior tibial artery, the lateral tarsal artery and the pedal arch are filled. **b** In phase 3 (20 s later), the peroneal artery as well as the proximal part of the posterior tibial artery, the dorsal pedal artery and the medial plantar artery are opacified. Note an early filling of the saphenous vein

and foot arteries was performed with at least two selective injections, each with 12–15-ml contrast agent (iodixamol, Visipaque 320, Nycomed-Amersham, Ismaning, Germany) to depict anteroposterior and lateral projections (Fig. 4). A flat-panel detector unit was used for intra-arterial angiography (Axiom artis dTA, Siemens, Forchheim, Germany).

## Image evaluation

All 3DceMRA and iaDSA examinations were retrospectively and consensually evaluated by two experienced ra-

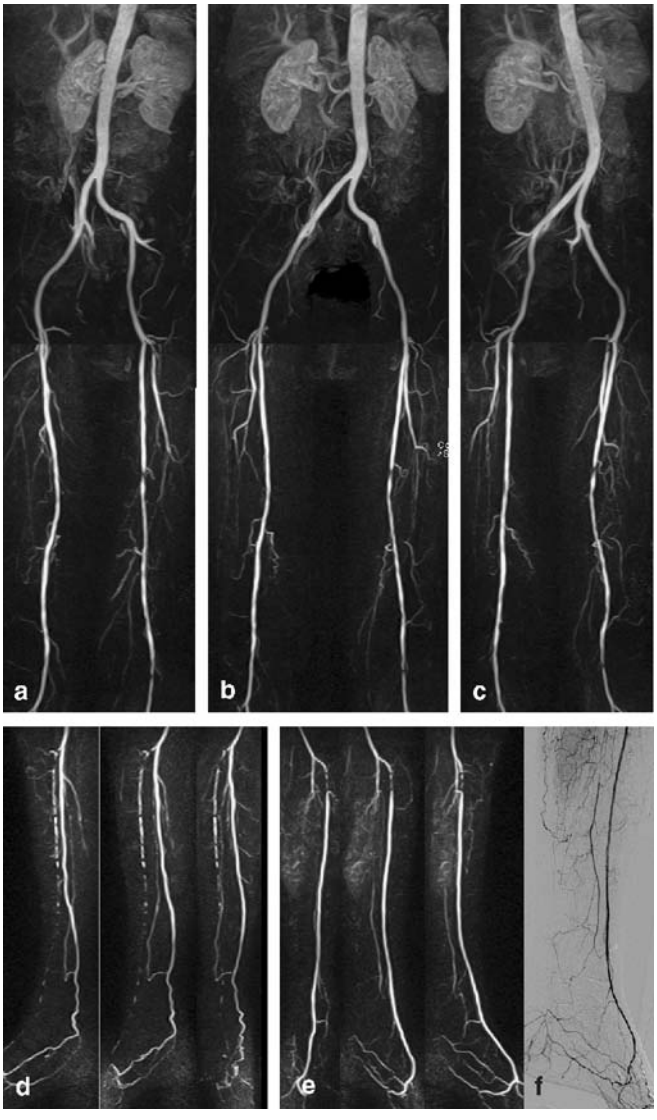


**Fig. 4** Modified hybrid 3DceMRA of a 77-year-old female suffering from claudication of her left side (Fontaine stage III). Comparison of findings in 3DceMRA and iaDSA. Aortofemoral bolus-chase 3DceMRA displayed in 45° oblique RAO (**a**), coronal (**b**) and 45° oblique LAO (**c**) maximum intensity projections. High-grade stenosis of the left deep femoral artery as well as intermediate stenoses of the left superficial femoral and the popliteal arteries. **d**–**e** Cruropedal time-resolved 3DceMRA, displayed in coronal, 45° oblique, and sagittal maximum intensity projections. On the *right side* (d), severe stenoses and segmental occlusions of the anterior tibial artery are present. Retrograde filling of the proximally stenosed peroneal artery. The posterior tibial artery and the plantar arteries are patent. On the left side (e), both the posterior tibial and the peroneal arteries are occluded. The anterior tibial artery is patent, with a high-grade stenosis proximally. Van Dongen's collaterals to the distal part of the peroneal artery are visible. The plantar arteries are filled via the dorsal pedal artery and the pedal arch. **f** Corresponding iaDSA image of the left lower limb acquired after successful PTA of the femoropopliteal stenoses. In comparison to 3DceMRA (see **e**), there are identical vascular findings in the iaDSA angiogram

diologists (R.S. & G.C.) blinded to all patient data. In a randomized order, MRA source and MIP images and iaDSA images were independently displayed on a PACS workstation (J-Vision, TIANI, Vienna, Austria) without any patient information. Minimum time delay between the different interpretation sessions was 7 days to avoid evaluation bias. For both 3DceMRA and iaDSA analysis, the arteries of the distal calf and foot were divided into eight segments: anterior tibial artery, posterior tibial artery, peroneal artery, dorsal pedal artery, medial plantar artery, lateral plantar artery, lateral tarsal artery, and plantar arch.

3DceMRA source images and maximum intensity projections of only the cruropedal station were analyzed in all 216 patients. Overall image quality was assessed with a four-point arterial interpretability score: 1=excellent, sharp arterial delineation in full length; 2=good, blurring of only a short arterial segment; 3=moderate, blurring of a long arterial segment; 4=poor, exact arterial delineation missing. The extent of overlaying veins was assessed with a three-point venous background score: 1=none, no veins visible; 2=moderate, veins present but arteries fully delineable; 3=severe, overlaying veins compromise arterial detection. Furthermore, enhanced soft-tissue areas independent of venous filling were evaluated at the feet.

The presence of background veins at the thigh and pelvic stations were evaluated in the bolus-chase MRA section. In the lower limbs of 69 patients assessed with both 3DceMRA and iaDSA imaging, stenoses of the cruropedal arteries were graded as "insignificant" (50% narrowing or less) or "significant" (greater than 50% narrowing, including occlusions). Of the six patients with bilateral treatment, only the first procedure was evaluated to ensure that each case entered the data only with one observation per vessel.

### Statistics

In the entire patient group, descriptive (counting) statistics were performed to rate image quality of the 3DceMRA technique exclusively including (1) arterial interpretability score, (2) venous background score, (3) frequency of enhanced soft-tissue areas, and (4) frequency of venous enhancement at the aorto-femoral regions. No interobserver agreement was measured.

The patient subgroups were evaluated with respect to demographical data (gender, age, and Fontaine's stages) applying the Mann-Whitney-U test for testing differences in continuous data, and the chi-square test for testing differences in frequencies. Differences were considered exploratively significant when $P$ values were $<0.05$.

In patient subgroup 1, sensitivity and specificity analysis of 3DceMRA findings was performed for each of the eight cruropedal arteries; therefore, comparisons were determined on the vessel-by-vessel basis (Table 3). IaDSA was set as the standard of reference for statistical analysis. Finally, the congruence between 3DceMRA and iaDSA was evaluated by counting the number of congruently assessed arteries in the sample of all vessel segments (Table 4). Ninety-five percent confidence ranges were calculated for the parameters of sensitivity, positive predictive value, specificity, and the negative predictive value as well as for the congruence analysis.

## Results

### Evaluation of only the ceMRA (entire patient group)

Using the arterial interpretability score at consensus reading, overall image quality of the cruropedal arteries was

**Table 3** Sensitivity and specificity analysis of ceMRA imaging for the differentiation of stenoses as "insignificant" (50% lumen narrowing or less) or "significant" (greater than 50% lumen narrowing and occlusions)

| Vessel segment | Sensitivity[a] | | Positive predictive value[b] | | Specificity[c] | | Negative predictive value[d] | |
|---|---|---|---|---|---|---|---|---|
| | No. (%) | (95% CI) | No. (%) | (95% CI) | No. (%) | (95% CI) | No. (%) | (95% CI) |
| Anterior tibial artery | 44/45 (98) | (88; 100) | 44/44 (100) | (90; 100) | 24/24 (100) | (82; 100) | 24/25 (96) | (80; 100) |
| Posterior tibial artery | 44/45 (98) | (88; 100) | 44/44 (100) | (90; 100) | 24/24 (100) | (82; 100) | 24/25 (96) | (80; 100) |
| Peroneal artery | 4/5 (80) | (28; 99) | 4/4 (100) | (28; 100) | 64/64 (100) | (93; 100) | 64/65 (98) | (92; 100) |
| Dorsal pedal artery | 19/20 (95) | (75; 100) | 19/19 (100) | (78; 100) | 49/49 (100) | (91; 100) | 49/50 (98) | (89; 100) |
| Medial plantar artery | 28/29 (97) | (82; 100) | 28/31 (90) | (74; 100) | 37/40 (93) | (80; 98) | 37/38 (97) | (86; 100) |
| Lateral plantar artery | 21/25 (84) | (64; 95) | 21/23 (91) | (72; 99) | 42/44 (95) | (85; 99) | 42/46 (91) | (79; 98) |
| Lateral tarsal artery | 31/31 (100) | (86; 100) | 31/31 (100) | (86; 100) | 38/38 (100) | (88; 100) | 38/38 (100) | (88; 100) |
| Plantar arch | 32/37 (86) | (71; 95) | 32/34 (94) | (80; 99) | 30/32 (94) | (79; 99) | 30/35 (86) | (70; 95) |

IaDSA findings are considered to be the standard of reference. Results are compared on a vessel-by-vessel basis. For each vessel, statistical values are listed as numbers of observations (No.), point estimators (%) as well as 95% confidence intervals (95% CI)

[a]Sensitivity means likelihood that 3DceMRA is correctly detecting significant stenoses and occlusions

[b]Positive predictive value means likelihood that significant stenoses and occlusions found in 3DceMRA are true

[c]Specificity means likelihood that 3DceMRA is correctly defining normals and nonsignificant stenoses

[d]Negative predictive value means likelihood that normals and nonsignificant stenoses found in 3DceMRA are true

**Table 4** Descriptive congruence analysis of 3DceMRA and iaDSA in imaging the cruropedal arteries

| Intra-individual vessels analysis | | Percentage of congruence between 3DceMRA and iaDSA | | |
|---|---|---|---|---|
| Vessels congruently imaged at each lower leg | Numbers(*n*) | Frequency (%) | Lower 95% confidence | Upper 95% confidence |
| 5/8 (62.5%) | 1/69 | 1% | 0% | 8% |
| 6/8 (75.0%) | 1/69 | 1% | 0% | 8% |
| 7/8 (87.5%) | 16/69 | 23% | 14% | 32% |
| 8/8 (100.0%) | 51/69 | 74% | 64% | 84% |

The congruence between both modalities is intra-individually counted in the patient subgroup 1 (*n*=69), i.e., diagnostic agreement in eight of eight cruropedal arteries (congruence of 100%) was observed in 74% of the sample yielding lower and upper 95% confidences of 64 and 84%, respectively

excellent in 136/216 cases (63%), good in 69/216 cases (32%), and moderate in 8/216 cases (4%). Image quality was considered poor in 3/216 cases (1%) due to motion-induced subtraction misregistration artifacts. One patient required a further MRI session for final diagnosis. In none of the 216 patients was additional X-ray angiographies carried out to reach definitive treatment decision.

Applying the venous background score, the distal calf and pedal arteries were assessed without any venous superimposition in 203/216 cases (94%), with moderate (Fig. 3b) and severe venous overlaying in 10/216 cases (5%) and in 3/216 cases (1%), respectively. In the aorto-femoral bolus-chase 3DceMRA, no venous enhancement was found in 169/216 cases (78%), and slightly enhanced veins in the remaining 47/216 cases (22%). Depiction of the pelvic and thigh arteries was never jeopardized.

Enhanced soft-tissue areas independent of venous filling was identified in 68/216 cases (31%; Fig. 2e). Based on the clinical presentation and findings in ceMRA imaging, treatment decisions were as follows. Conservative regimes were ordered in 46/216 patients, and surgical procedures (bypass grafting, vascular endoprothesis) were performed in 66/216 patients. According to the TASC criteria, 104/216 patients were scheduled for percutaneous transluminal angioplasty of the iliacal, femoropopliteal or crural vessel segments. From the interventional cases, 69/104 catheter angiograms of the cruropedal station were available (patient subgroup 1).

### CeMRA evaluation of the cruropedal arteries in comparison to iaDSA (patient subgroup 1)

In subgroup 1 (69/216 patients), the cruropedal arteries were examined with ceMRA as well as with catheter angiography. With regard to demographical data, there were no differences found between subgroup 1 and the remaining 147/216 patients (subgroup 2) for gender, age, or for the Fontaine's stages (Table 1).

Agreement between 3DceMRA and iaDSA was intra-individually tested for each of eight cruropedal arteries. With iaDSA as the standard of reference, the modified hybrid dual-bolus 3DceMRA yielded observed sensitivity rates between 80% for the peroneal artery and 100% for the lateral tarsal artery. Observed specificity values ranged from 93% for the medial plantar artery to 100% in the anterior and posterior tibial arteries. Positive predictive values as well as negative predictive values were predominantly within the same ranges. Confidence ranges are specified in Table 3. Except for the lateral tarsal artery, which was correctly diagnosed with 3DceMRA in all cases, there was a tendency for better congruence of both modalities at the more proximal (crural) vessel segments.

Complete intra-individual agreement for all (8/8) vessel segments was seen in 51/69 cases yielding a congruence rate of 74% with lower and upper 95% confidence intervals of 64% and 84%, respectively (Fig. 4). Partial (7/8) agreement was observed in 16 cases (congruence 23%, 95% confidence intervals of 14 and 32%), whereas 6/8 and 5/8 congruence was counted for one case each (Table 4).

Discrepant imaging findings in at least one vessel segment were evident in 18/69 cases (26%). In eight cruropedal arteries, the stenotic degree was more severely assessed with 3DceMRA than with iaDSA (false positive findings). Another 13 peripheral segments showed a lesser degree of stenoses in 3DceMRA as compared to iaDSA (false negative findings). In eight of these patents, 3DceMRA displayed at least one patent vessel which was not visible in iaDSA. Therefore, these cases were judged as "false negatives" in 3DceMRA imaging. In the remaining five cases, the stenotic degree was underestimated in regards to 3DceMRA. Detailed imaging results of the cruropedal vessels are summarized in Table 3. Finally, the length of four occlusions in the calf and foot regions was depicted significantly shorter using 3DceMRA in comparison to iaDSA.

## Discussion

In standard single-bolus 3DceMRA, depiction of the cruropedal vessels is challenging due to fundamentally different requirements for temporal and spatial resolution. When applying the craniocaudal bolus-chase order, about 5–25% of all 3DceMRA examinations are of suboptimal diagnostic quality due to venous contamination of the calves [1, 2,

23]. Furthermore, this acquisition approach often fails to completely cover the feet and thus "cuts off" the pedal vasculature. By modifying the dual-bolus 3DceMRA strategy, the entire infrapopliteal vasculature including the pedal arteries becomes assessable in high-resolution angiograms (Fig. 5). Our refined technique is different from previously described hybrid MRA approaches for several reasons:

– Acquisition volumes of the feet were angled to sagittal orientation to fully cover the vessels of the distal calf and foot down to the pedal arches. Formerly, this technique was applied for dedicated 3D imaging of the pedal vessels alone [25, 26]. Sagittal slab orientation is benificial for vessel assessment at the rectangular junction of the ankle for three reasons. Firstly, the calf and pedal arteries become accessible in a continuous way of presentation. This anatomic visualization is crucial for planning distal bypass grafts in patients with severely diseased calf arteries. Secondly, partial-volume effects may be decreased in slice direction by aligning the slab orientation according to the vessel topography. The pedal vessels are depicted with improved in-plane

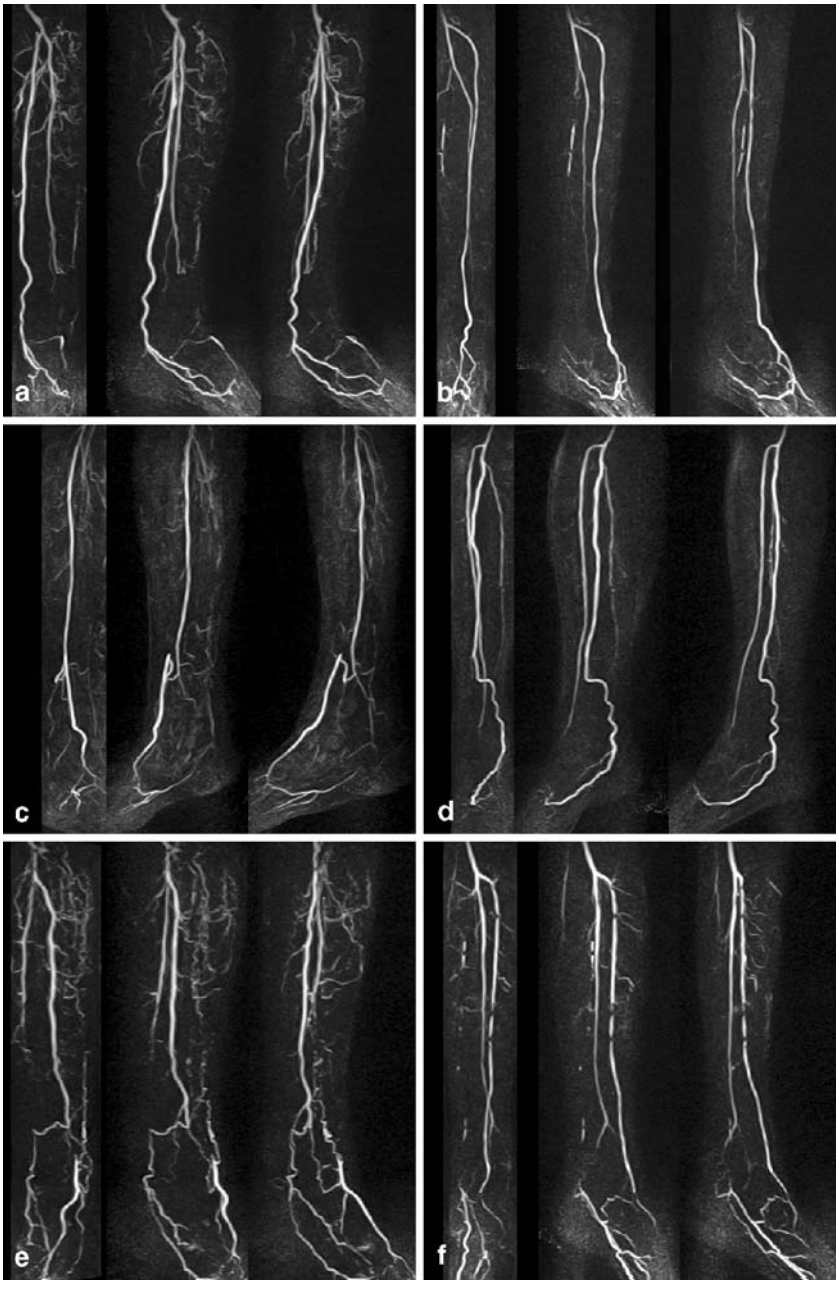


**Fig. 5** Image collection of different vascularity patterns in the cruropedal area. Cruropedal time-resolved 3DceMRA's of six patients examined with the modified hybrid 3DceMRA technique. **a** Occlusion of the anterior tibial artery. The posterior tibial artery as well as the plantar vessels are patent. A collateral to the dorsal pedal artery is visible. **b** Occlusion of the posterior tibial artery. The anterior tibial and the dorsal pedal arteries as well as the plantar arch are patent. **c** Proximal occlusions of both tibial arteries. Van Dongen's collaterals run from the patent peroneal artery mainly to the dorsal pedal artery. **d** Distal occlusions of both tibial arteries. A Van Dongen's collateral runs from the patent peroneal artery to the distal tibial artery which feeds the plantar vessels. **e** Occlusions of both tibial arteries. Several collaterals (Van Dongen) run from the peroneal artery to the plantar vessels as well as to the dorsal pedal artery. **f** Complex collateral pathways of the pedal vasculature. Occlusion of the posterior tibial artery. Multisegmental stenoses of the anterior tibial artery which fills the distally occluded dorsal pedal artery. Collaterals to the plantar arteries have developed

resolution in sagittal orientation [25, 26], whereas the tibial trifurcation is best visualized by means of a coronal slab [28]. Thirdly, acquiring two side-different slabs is very timesaving, because the median volume between the calves, which is redundant for vessel imaging, is left blank. In recent literature, another solution was to extend the distal coronal slab in an anteroposterior direction by more than doubling the number of partitions [4, 7, 10, 20]. Obviously, this ceMRA technique offers the opportunity of simultaneously filling the calf veins during the long acquisition time.

– Mean contrast travel time from an antecubital vein to the midcalf arteries has been determined at about 30 s with a wide variation, depending on factors like age, left ventricular function, the presence of an aortic aneurysm, and peripheral inflammatory disease [13, 14]. After contrast arrival at the calves, there is only a short passage time of about 7 s that has been estimated [14], followed by a fast arterial-venous transit [13]. Late acquisition of the cruropedal vessels may increase the likelihood of venous contamination in cranio-caudal, single-bolus 3DceMRA [10, 24]. To overcome this limitation, we depicted the cruropedal arteries first with a time-resolved, multiphase 3D sequence over 1 min and 40 s and a fixed start delay of 15 s (Fig. 3). This approach always covers the "arterial window" during the first passage of the contrast bolus, and therefore provides reliably pure arterial-phase images [15, 21, 22, 24, 25]. According to our experience, exact MR fluoroscopic detection of the bolus arrival is not promising in severely diseased peripheral arteries, mainly due to the small vessel sizes and side-different transit times.
– For sufficient coverage of the bolus length during its contrast passage through the calf arteries, we applied a sensitivity-encoding sequence [19, 20, 29] in combination with a multichannel phased-array coil to increase acquisition speed of the cruropedal station. The use of the phased-array coil allows SENSE application in all peripheral stations with a free choice of the acquisition plane and the phase encoding direction. A centric k-space filling order was used for early encoding of the contrast information, thus covering the arterial arrival in time and diminishing venous enhancement [10].
– Besides the requirements of proper temporal resolution, depiction of the cruropedal arteries is challenging due to the small vessel sizes [7]. The vessel signal is further decreased when SENSE imaging is applied [20, 29]. Generally, vascular signal-to-noise ratio (SNR) can be improved in MR angiography by using contrast agents either of a higher concentration like gadobutrol [30] or of an increased relaxivity like gadopentate [22, 31].

Three other techniques have been described to obtain higher temporal resolution for the depiction of peripheral vessels. One approach uses a time-resolved 2D sequence to acquire projectional images of the cruropedal station every 2 s [23]. There are some drawbacks of the 2D acquisition method. Firstly, the image information is projectional, and therefore does not allow for reconstruction from different views. Secondly, image reconstruction every 2 s is very time-consuming. The second technique, the so-called TRICKS modification (Time resolved imaging of contrast kinetics), is a fast data sampling method in MR angiography [32, 33]. With TRICKS, which was not implemented in our sequence file, time-resolution can drastically be improved by updating the contrast information in the central part of the k-space every few seconds, whereas the high-spatial-frequency information of the k-space periphery is less frequently sampled after the first contrast passage [32, 33]. In our study, we used the third technique, the GRAPPA technique, to further increase acquisition speed. Although it lowers the SNR, sensitivity-encoded 3DceMRA has been assessed as significantly improving the depiction of peripheral arteries mainly by avoiding venous overlay [19, 20, 29]. A synergistic approach for attaining high-quality and time-resolved images of the distal run-off arteries would be the combined application of (1) sagittal slab orientation, (2) SENSE imaging, (3) k-space zero-filling, and (4) the TRICKS technique.

Analysis of stenosis quantification with the use of ceMRA revealed excellent correlation with the values derived in iaDSA. However, in the assessment of occluded vessel segments, we found eight patent run-off arteries which were clearly visible in hybrid dual-bolus 3DceMRA, but not seen on iaDSA. In several studies, 3DceMRA has been proved superior to iaDSA for the identification of patent run-off vessel segments of the calves [12, 19, 29] and the feet [25, 26]. Moreover, 3DceMRA depicts the exact ("true") length of an occluded vessel segment, probably by a time-dependent and retrograde filling of the postocclusion segment via collaterals [17] (Fig. 5e and f). For the assessment of infrapopliteal lesions, contrast-enhanced multislice spiral CT angiography has been considered problematic due to the small vessel size [34] and intramural calcifications which may disable stenosis quantification [35].

Other than adding the pedal station at the end of a standard single-bolus 3DceMRA [24] or increasing the distal slab volume [4, 7, 10, 20], we preferred to acquire the cruropedal data set first, because the diagnostic accuracy of the biphasic, dual-bolus approach has been proven to be higher than the standard single-bolus 3DceMRA [21–23]. As reported with the step-by-step and the hybrid MRA techniques [17, 21, 36, 37], the previously applied contrast agent did not hamper image interpretability of the iliacal and femoropopliteal stations in any of our patients because the venous background enhancement was sufficiently suppressed by the "mask" data sets (Figs. 2a–c and 4a–c). However, we observed areas with focal or diffuse soft-tissue enhancement patterns in about 32% of all feet. These

hyperemic areas are frequently seen on late phases of time-resolved 3DceMRA images in diabetic patients suffering from cellulites, gangrene, or ulceration [38].

We acknowledge some limitations of the present study. Firstly, a nonselected patient cohort of our routine work-up was evaluated with a high frequency of advanced PVD stages, while normal findings were missing. Secondly, the study design was a retrospective one. Therefore, only parts of the 3DceMRA examinations were comparable with findings in catheter angiography due to the limited availability of iaDSA images. However, no significant differences were found in the patient data of the subgroups, and especially the PVD distribution was similar. Thirdly, we used a simple two-point scale for assessing vessel stenoses. The high number of occluded run-off arteries in our study population may account for an artificial over-estimation of the diagnostic quality of 3DceMRA. Fourth, the acquisition order was alternating, not interleaved for both cruropedal slabs. An interleaved order for simultaneously acquiring both extremities without extending the acquisition time was not implemented on our scanners. Finally, we used two scanner platforms with different gradient strengths, resulting in different scan parameters.

## Conclusion

Most of the limitations of standard single-bolus 3DceMRA in visualizing the cruropedal arteries have been resolved by the modified scan protocol presented in this paper. This refined examination strategy, which is simple to perform in clinical practice, provides high-quality images of the entire peripheral vasculature and will, therefore, increase the clinical relevance of 3DceMRA as the first-line angiographic examination for planning and controlling revascularization procedures of the lower limbs.

**Acknowledgements** Ulrich Stefenelli, Institute of Statistics, Wuerzburg (Germany), is kindly acknowledged for analyzing the data statistically. We are in debt to our radiological technicians (Janina Erck, Franziska Hahn, Gerd Metz, Birgit Pfaff, Silke Raeder, Sonja Schmitt, Marco Straub, Ulrike Thielicke) who passionately and knowledgably performed the MR angiograms.

## References

1. Busch HP, Hoffmann HG, Rock J, Schneider C (2001) MR angiography of pelvic and leg vessels with automatic table movement technique ("Mobi-Trak"): clinical experience with 450 studies. Rofo Fortschr Geb Rontgenstr Neuen Bildgeb Verfahr 173:405–409
2. Lenhart M, Finkenzeller T, Paetzel C, Strotzer M, Mann S, Djavidani B, Nitz WR, Link J, Feuerbach S, Kasprzak P (2002) Contrast-enhanced MR angiography in the routine work-up of the lower extremity arteries. Rofo Fortschr Geb Rontgenstr Neuen Bildgeb Verfahr 174:1289–1295
3. Loewe C, Schoder M, Rand T, Hoffmann U, Sailer J, Kos T, Lammer J, Thurnher S (2002) Peripheral vascular occlusive disease: evaluation with contrast-enhanced moving-bed MR angiography versus digital subtraction angiography in 106 patients. AJR Am J Roentgenol 179:1013–1021
4. Meaney JFM (2003) Magnetic resonance angiography of the peripheral arteries: current status. Eur Radiol 13:836–852
5. Wang YI, Lee HM, Khilnani NM, Trost DW, Jagust MB, Winchester PA, Sos HL, Sostman HD (1998) Bolus-chase MR digital subtraction angiography in the lower extremity. Radiology 207:263–269
6. Prince MR, Chenevert TL, Foo TK, Londy FJ, Ward JS, Maki JH (1997) Contrast-enhanced abdominal MR angiography: optimization of imaging delay time by automating the detection of contrast material arrival in the aorta. Radiology 203:109–114
7. Leiner T, Ho KYJAM, Nelemans PJ, de Haan MW, van Engelshoven JMA (2000) Three-dimensional contrast-enhanced moving-bed infusion-tracking (MoBi-Track) peripheral MR angiography with flexible choice of imaging parameters for each field of view. J Magn Reson Imaging 11:368–377
8. Janka R, Fellner F, Fellner C, Requardt M, Reykowski A, Lang W, Wutke R, Bautz W (2000) Dedicated phased-array coil for peripheral MRA. Eur Radiol 10:1745–1749
9. Huber A, Scheidler J, Wintersperger B, Baur A, Schmidt M, Requardt M, Holzknecht N, Helmberger T, Billing A, Reiser M (2003) Moving-table MR angiography of the peripheral runoff vessels: comparison of body coil and dedicated phased array coil systems. AJR Am J Roentgenol 180:1365–1373
10. Leiner T, Nijenhuis RJ, Maki JH, Lemaire E, Hoogeveen R, van Engelshoven JMA (2004) Use of a three-station phased array coil to improve peripheral contrast-enhanced magnetic resonance angiography. J Magn Reson Imaging 20:417–425
11. Rofsky NM, Johnson G, Adelman MA, Rosen RJ, Krinsky GA, Weinreb JC (1997) Peripheral vascular disease evaluated with reduced-dose gadolinium-enhanced MR angiography. Radiology 205:163–169
12. Steffens JC, Schafer FK, Oberscheid B, Link J, Jahnke T, Heller M, Brossmann J (2003) Bolus-chasing contrast-enhanced 3D MRA of the lower extremity: comparison with intraarterial DSA. Acta Radiol 44:185–192
13. Wang Y, Chen CZ, Chabra SG, Winchester PA, Khilnani NM, Watts R, Bush L Jr, Kent CK, Prince MR (2002) Bolus arterial-venous transit in the lower extremity and venous contamination in bolus chase three-dimensional magnetic resonance angiography. Invest Radiol 37:458–463
14. Prince MR, Chabra SG, Watts R, Chen CZ, Winchester PA, Khilnani NM, Trost D, Bush HA, Kent KC, Wang Y (2002) Contrast material travel times in patients undergoing peripheral MR angiography. Radiology 224:55–61
15. Schmitt R, Christopoulos G, Brunner S, Froehner S, Dobritz M, Fellner F (2001) MR angiography of pelvic and leg arteries: initiation with time-resolved data acquisition of the lower legs. Roentgenpraxis 54:83–92

16. Herborn CU, Ajaj W, Goyen M, Massing S, Ruehm SG, Debatin JF (2004) Peripheral vasculature: whole-body MR angiography with midfemoral venous compression—initial experience. Radiology 230:872–878
17. Huber A, Heuck A, Baur A, Helmberger T, Waggershauser T, Billing A, Heiss M, Petsch R, Reiser M (2000) Dynamic contrast-enhanced MR angiography from the distal aorta to the ankle joint with a step-by-step technique. AJR Am J Roentgenol 175:1291–1298
18. Morasch MD, Collins J, Pereles FS, Carr JC, Eskandari MK, Pearce WH, Finn JP (2003) Lower extremity stepping-table magnetic resonance angiography with multilevel contrast timing and segmented contrast infusion. J Vasc Surg 37:62–71
19. Bezooijen R, van den Bosch HC, Tielbeek AV, Thelissen GR, Visser K, Hunink MG, Duijm LE, Wondergem J, Buth J, Cuypers PW (2004) Peripheral arterial disease: sensitivity-encoded multiposition MR angiography compared with intraarterial angiography and conventional multiposition MR angiography. Radiology 231:263–271
20. de Vries M, Nijenhuis RJ, Hoogeveen RM, de Haan MW, van Engelshoven JMA, Leiner T (2005) Contrast-enhanced peripheral MR angiography using SENSE in multiple stations: feasibility study. J Magn Reson Imaging 21:37–45
21. Binkert CA, Baker PD, Petersen BD, Szumowski J, Kaufman JA (2004) Peripheral vascular disease: blinded study of dedicated calf MR angiography versus standard bolus-chase MR angiography and film hard-copy angiography. Radiology 232:860–866
22. von Kalle T, Gerlach A, Hatopp A, Klinger S, Prodehl P, Arlart IP (2004) Contrast-enhanced MR angiography (CEMRA) in peripheral arterial occlusive disease (PAOD): conventional moving table technique versus hybrid technique. Rofo Fortschr Geb Rontgenstr Neuen Bildgeb Verfahr 176:62–69
23. Wang Y, Winchester PA, Khilnani NM, Lee HM, Watts R, Trost DW, Bush HL Jr, Kent KC, Prince MR (2001) Contrast-enhanced peripheral MR angiography from the abdominal aorta to the pedal arteries: combined dynamic two-dimensional and bolus-chase three-dimensional acquisitions. Invest Radiol 36:170–177
24. Konkus CJ, Czum JM, Jacobacci JT (2002) Contrast-enhanced MR angiography of the aorta and lower extremities with routine inclusion of the feet. AJR Am J Roentgenol 179:115–117
25. Kreitner KF, Kalden P, Neufang A, Düber C, Krummenauer F, Küstner E, Laub G, Thelen M (2000) Diabetes and peripheral arterial occlusive disease: prospective comparison of contrast-enhanced three-dimensional MR angiography with conventional digital subtraction angiography. AJR Am J Roentgenol 174:171–179
26. Cronberg CN, Sjoberg S, Albrechtsson U, Leander P, Lindh M, Norgren L, Danielsson P, Sonesson B, Larsson EM (2003) Peripheral arterial disease. Contrast-enhanced 3D MR angiography of the lower leg and foot compared with conventional angiography. Acta Radiol 44:59–66
27. Fellner FA, Requardt M, Lang W, Fellner C, Bautz W, Cavallaro A (2003) Peripheral vessels: MR angiography with dedicated phased-array coil with large-field-of-view adapter feasibility study. Radiology 228:284–289
28. Yamashita Y, Mitsuzaki K, Ogata I, Takahashi M, Hiai Y (1998) Three-dimensional high-resolution dynamic contrast-enhanced MR angiography of the pelvis and lower extremities with use of a phased array coil and subtraction: diagnostic accuracy. J Magn Reson Imaging 8:1066–1072
29. Maki JH, Wilson GJ, Eubank WB, Hoogeveen RM (2002) Utilizing SENSE to achieve lower station submillimeter isotropic resolution and minimal venous enhancement in peripheral MR angiography. J Magn Reson Imaging 15:484–491
30. Hentsch A, Aschauer MA, Balzer JO, Brossmann J, Busch HP, Davis K, Douek P, Ebner F, van Engelshoven JMA, Gregor M, Kersting C, Knüsel PR, Leen E, Leiner T, Loewe C, McPherson S, Reimer P, Schäfer FKW, Taupitz M, Thurnher SA, Tombach B, Wegener R, Weishaupt D, Meaney JFM (2003) Gadobutrol-enhanced moving-table magnetic resonance angiography in patients with peripheral vascular disease: a prospective, multi-entre blinded comparison with digital subtraction angiography. Eur Radiol 13:2103–2114
31. Goyen M, Debatin JF (2003) Gadobenate dimeglumine (MultiHance) for magnetic resonance angiography: review of the literature. Eur Radiol 13(Suppl 3):N19–N27
32. Swan JS, Carroll TJ, Kennell TW, Heisey DM, Korosec FR, Frayne R, Mistretta CA, Grist TM (2002) Time-resolved three-dimensional contrast-enhanced MR angiography of the peripheral vessels. Radiology 225: 43–52
33. Du J, Carroll TJ, Wagner HJ, Vigen K, Fain SB, Block WF, Korosec FR, Grist TM, Mistretta CA (2002) Time-resolved, undersampled projection reconstruction imaging for high-resolution CE-MRA of the distal runoff vessels. Magn Reson Med 48:516–522
34. Portugaller HR, Schoellnast H, Hausegger KA, Tiesenhausen K, Amann W, Berghold A (2004) Multislice spiral CT angiography in peripheral arterial occlusive disease: a valuable tool in detecting significant arterial lumen narrowing? Eur Radiol 14:1681–1687
35. Catalano C, Napoli A, Fraioli F, Venditti F, Votta V, Passariello R (2003) Multidetector-row CT angiography of the infrarenal aortic and lower extremities arterial disease. Eur Radiol 13: M88–M93
36. Janka R, Fellner FA, Fellner C, Lang W, Requardt M, Wutke R, Bautz WA (2000) A hybrid technique for the automatic floating table MRA of peripheral arteries using a dedicated phased-array coil combination. Rofo Fortschr Geb Rontgenstr Neuen Bildgeb Verfahr 172:477–481
37. Hany TF, Carroll TJ, Omary RA, Esparza-Coss E, Korosec FR, Mistretta CA, Grist TM (2001) Aorta and runoff vessels: single-injection MR angiography with automated table movement compared with multiinjection time-resolved MR angiography—initial results. Radiology 221:266–272
38. Zhang HL, Kent KC, Bush HL, Winchester PA, Watts R, Wang Y, Prince MR (2004) Soft tissue enhancement on time-resolved peripheral magnetic resonance angiography. J Magn Reson Imaging 19:590–597